April 2007

MEX-3 BINDS TO A CONSERVED FRAGMENT OF THE

David Mark Moquin
Worcester Polytechnic Institute

MQP-BC-DSA-4051

MEX-3 BINDS TO A CONSERVED FRAGMENT OF THE NOS-2 3'-UNTRANSLATED REGION

A Major Qualifying Project Report

Submitted to the Faculty of the

WORCESTER POLYTECHNIC INSTITUTE

in partial fulfillment of the requirements for the

Degree of Bachelor of Science

in

Biochemistry

by

David Moquin

April 26, 2007

APPROVED:

Sean Ryder, Ph.D.
Biochemistry and Mol Pharmacology
Umass Medical Center
Major Advisor

David Adams, Ph.D.
Biology and Biotechnology
WPI Project Advisor

ABSTRACT

Normal development during early embryogenesis in *Caenorhabditis elegans* is contingent upon both the temporal and spatial expression of several mRNAs. In the early embryo no transcription takes place, so the asymmetric expression of cell-fate determinants is reliant on post-transcriptional regulators. MEX-3 is an RNA-binding protein containing two KH-domains that is expressed in the proximal gonad arm and the anterior blastomeres and P granules in the early embryo. In this MQP, EMSAs and titration fluorescence polarization were employed to test the binding specificity of MEX-3 to the 3' UTR of *nos-2* mRNA. This MQP provides *in vitro* evidence that MEX-3 binds to domain subC of the 3'-UTR of *nos-2*, and establishes a basis for subsequent *in vivo* experiments which will test for MEX-3's role as a post-transcriptional regulator of *nos-2*.

TABLE OF CONTENTS

ACKNOWLEDGEMENTS

I would like to thank Dr. Sean Ryder for providing me with this great undergraduate research experience by providing me with an interesting project, the laboratory space needed to conduct my research, and helping me with editing the report. I would like to thank John Pagano for spending his time teaching me the assays and the theory behind them during a time when he was very busy getting prepared for his PhD qualifying exam. I would like to thank Dr. David Adams for helping me initiate this project as well as providing assistance with editing the report.

BACKGROUND

C. elegans Embryogenesis

In order for proper development during early embryogenesis in *C. elegans* to occur, the temporal and spatial regulation of specific mRNAs is required. Due to the fact that virtually no transcription occurs in the early embryo, post transcriptional mechanisms of regulation are utilized in order to regulate the expression of specific cell fate determinants. Varying post-transcriptional mechanisms are employed in the early embryo, such as repression via protein binding to the 3'-UTR of specific mRNAs encoding cell fate determinants, and alterations in mRNA stability (Kuersten and Goodwin, 2003).

The initial antero-posterior polarity of the zygote is established upon entry of the sperm pronucleus which leads to the subsequent asymmetric distribution of maternal mRNA and proteins. During early embryogenesis, the cells divide asymmetrically, and the first cell division gives rise to a stem cell (P1) and a founder cell (AB) (Fig. 1). The stem cell (P1) is undifferentiated, while the founder cell (AB) gives rise to specific differentiated daughter cells. During the second cell division of embryogenesis, the AB cell division occurs perpendicular to the anterior-posterior axis, and produces the daughters AB.a and AB.p, while the P1 cell division occurs transversely and produces the daughters EMS and P2. Division of posterior blastomeres produces both a founder cell and a stem cell, while the division of anterior blastomeres only produces founder cells thus the posterior blastomeres are responsible for perpetuating the stem cell linage during embryogenesis (Wormbook, 2005).

Cell specification varies between the differing blastomeres in the early embryo. While some cells such as P1 are specified in an autonomous manner, others such as AB are specified in a conditional manner. This means that the proper specification of the P1 blastomere is reliant on internal cytoplasmic factors and not signals from neighboring cells, while the proper specification of the AB blastomere is reliant on signals from neighboring cells in addition to internal cytoplasmic factors (Wormbook, 2005).

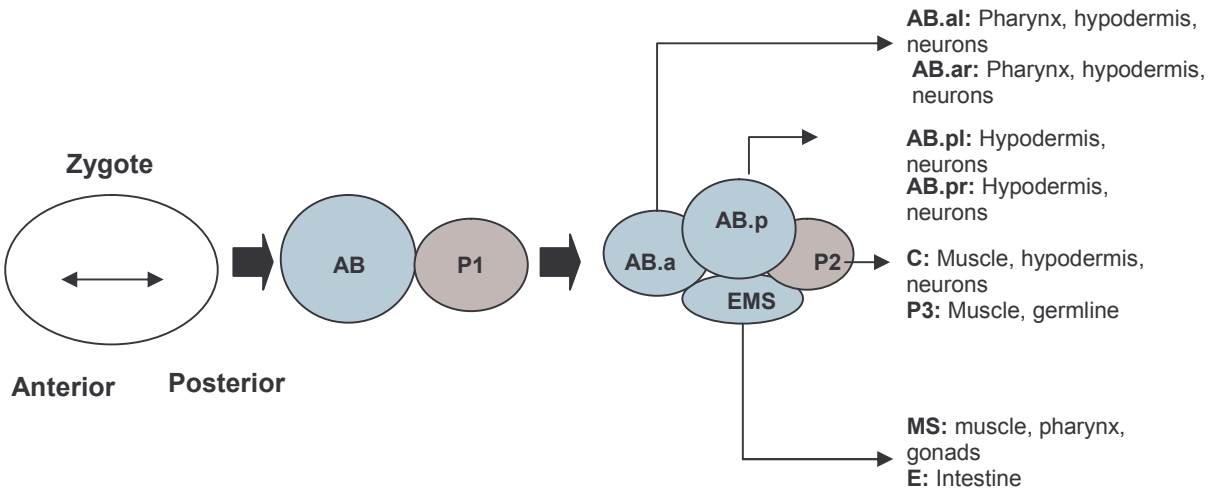

Figure 1: Early Embryogenesis in *C. elegans.*

Two major classes of maternally expressed genes are crucial for normal patterning in the embryo. The early acting polarity genes are important both in establishing and maintaining polarity in the early embryo, while the cell fate determinants are important for specifying cell linages. The *par* genes are examples of early acting polarity genes because loss of function mutations of these genes result in the elimination of cell polarities in the early embryo which translates to defects in cell cycle timing, loss of asymmetric cell size, defects in spindle orientation, and loss of asymmetric distribution of cell fate determinants. Cell fate determinants

include transmembrane proteins involved in cell signaling and transcription factors (Huang et al., 2002). Acting between the early acting polarity genes and the cell fate determinants are specific regulators.

MEX-3

PAL-1 offers a specific example of how a cell-fate determinant's expression is translationally regulated and in result conveys the information provided by the asymmetric distribution of specific regulators to the cell-fate determinants temporal and spatial expression. PAL-1 is a homeodomain protein which functions as a determinant of posterior blastomere fate. *pal-1* mRNA is distributed symmetrically throughout the early embryo; however, its expression is restricted to the posterior blastomeres during the four cell stage (Waring and Kenyon, 1990; Hunter and Kenyon, 1996). MEX-3 is an RNA binding protein which contains two KH-domains. MEX-3 expression is restricted to the anterior blastomeres during early embryogenesis which is complementary to PAL-1 expression (Mootz et al., 2004). Genetic studies provide evidence that MEX-3 is required for the temporal and spatial expression of PAL-1, and may directly regulate PAL-1 via binding the *pal-1* 3'-UTR (Hunter and Kenyon, 1996). Experimental evidence suggests that the mechanism for repression via the 3'-UTR occurs by preventing the interaction between eIF4E with eIF4G which is necessary for the recruitment of the small ribosomal subunit (Mootz et al., 2004).

On a phenotypic level, after the first cleavage in wild-type *C. elegans* embryos, muscles can only be produced by the posterior blastomere linage. However, embryos with maternal-effect lethal mutations in the *mex-3* gene result in anterior blastomeres that adopt C-like fates and thus inappropriately give rise to muscle cells (Draper et al, 1996). In result, embryos that are

mex-3 mutants produce muscle tissue and hypodermal tissue where pharyngeal and nervous tissue would normally be located in wild type embryos (Fig. 2).

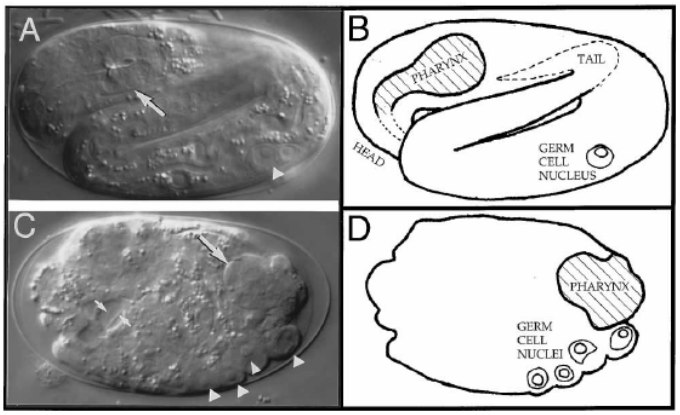

Figure 2: (A and C) photomicrographs of wild-type *C. elegans* embryo and *mex-3* mutant embryo, respectively. (B and D) Schematic diagrams of (A) and (C) (Draper et al., 1996).

Both *mex-3* mRNA and MEX-3 protein are asymmetrically distributed in the early embryo. *mex-3* mRNA is symmetrically distributed throughout the early 1-cell stage embryo, but towards the later 1-cell stage it begins to be localized to the anterior portion of the embryo. As a result, during the two-cell and four-cell stage, *mex-3* mRNA is localized to the anterior blastomeres. *mex-3* mRNA is no longer found in the anterior blastomeres after the four-cell stage. The patterning of MEX-3 protein is similar with its localization to the anterior blastomeres during early embryogenesis and also disappearance after the four-cell stage (Draper et al., 1996).

P-granules are ribonucleoprotein complexes where various mRNAs and protein are localized (Wormbook, 2005). They are segregated to the primordial germ cell line and thus are thought to be necessary for specifying germ cells in the embryo; however, the mechanism of this specification needs to be further elucidated. MEX-3 protein is also localized to the P-granules in P1, P2, P3, and P4 blastomeres. MEX-3 protein was not shown to be localized to the P-granules in the gonad or P-granules during later stages of embryogenesis. This could be attributed to the fact that MEX-3 is not localized to these P-granules during the aforementioned times; however,

this has not been validated because the MEX-3 epitope may have been masked during these stages of development (Draper et al., 1996).

It has been demonstrated through analysis of *mex-3* mutant embryos that MEX-3 is required for the proper development of P3. In *mex-3* mutants, the P3 daughters (P4 and D) both produce daughters that are characteristic of P4, suggesting that D is adopting the fate of P4. As a result, there is a correlation between the appropriate development of P3 and MEX-3's association with P-granules (Draper et al., 1996).

Experimental evidence suggests that MEX-3 may be regulated by MEX-5, MEX-6, and SPN-4 and thus aid in the asymmetric distribution of PAL-1 in the early embryo. MEX-5 and MEX-6 both contain two CCCH zinc finger motifs and their amino acid sequences are 70% identical (Schubert et al., 2000). Genetic studies suggest that MEX-5 and MEX-6 convey the asymmetric distribution information provided by the *par* genes to the correct temporal and spatial expression of PAL-1 (Bowerman, 1998; Huang et al., 2002). PAR-1 is a protein kinase which is localized to the posterior blastomeres in the early embryo. MEX-3's expression is restricted to the anterior blastomere's possibly through the repression of MEX-5 and MEX-6 activity in the posterior blastomere due to the action of PAR-1. Additionally, the absence of PAR-1 expression in the anterior blastomeres results in MEX-5 and MEX-6 activity which promote MEX-3's translational repression of *pal-1* (Fig. 3). Another protein believed to be important for the patterning of PAL-1 expression is SPN-4. SPN-4 is a protein which contains an RNA recognition motif and is thought to keep MEX-3 protein levels low in the posterior blastomeres and thus aid in the expression of PAL-1 in the posterior blastomeres (Huang et al., 2002).

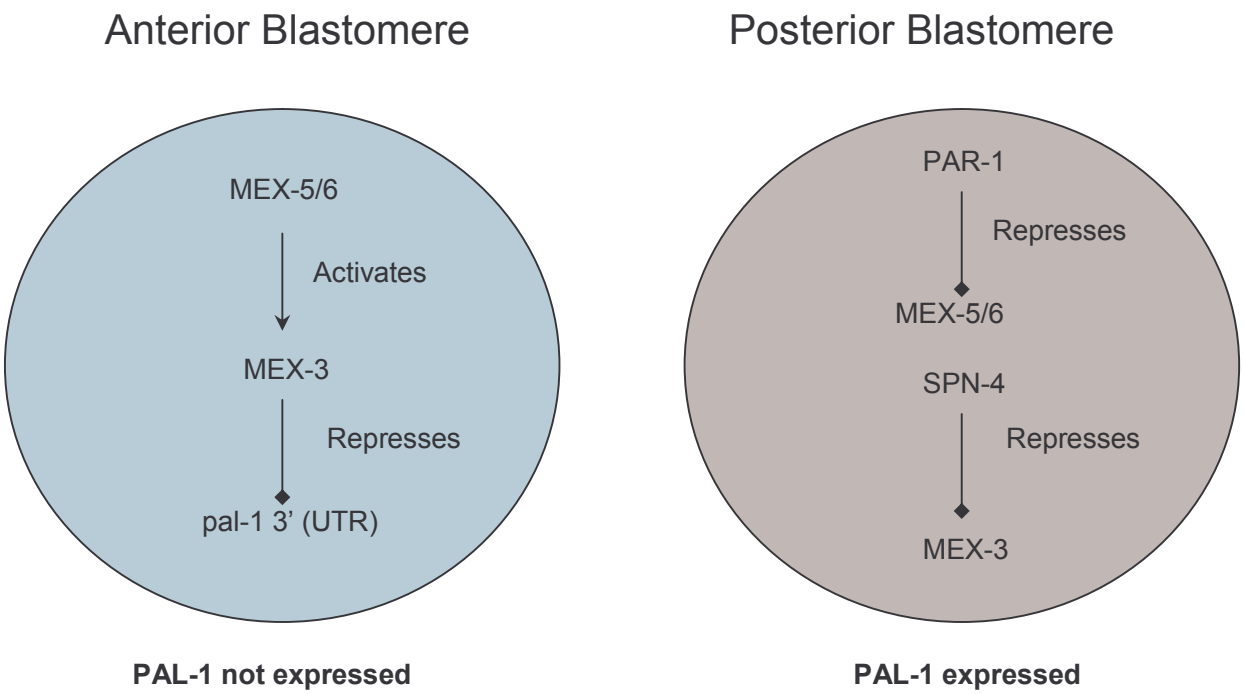

Figure 3: Cascade of factors that act in the repression of PAL-1 in anterior blastomeres.

Studies also show that MEX-3 is an important post-transcriptional regulator during germ cell development in the gonad. MEX-3 and GLD-1 are expressed in different portions of the gonad, with MEX-3 expression localized to the proximal gonad arm and GLD-1 expression localized to the distal gonad arm. Interestingly, the *gld-1;mex-3* double mutant phenotype has led to the discovery of the first tetratoma in invertebrates. Previously, tetratomas were only found in higher eukaryotes and were characterized by the spontaneous development of an egg without the fusion of the sperm which yields a mass of various types of somatic cells. The double mutant phenotype was a mass of disorganized somatic cells in the gonad that had transdifferentiated from germ cells. Specifically, the mass of somatic cells has been identified as neurons, intestine, and muscle (Seydoux and Braun, 2006). Although MEX-3 and GLD-1 are important for translational repression of *pal-1* mRNA in the gonad, it has yet to be determined

what specifically contributes to the transdifferentiation. Such speculations include a combination of PAL-1 and other cell fate determinants being inappropriately expressed in the gonad as well as a defect that allows the germ cells to be receptive of these changes in protein expression. The latter portion of the speculation is substantiated by GLD-1's role in regulating the shift from transcriptional active to transcriptional inactive phases during meiosis in the gonad. Inability of a developing germ cell to switch phases may cause it to be receptive to the inappropriately expressed cell fate determinants and result in transdifferentiation.

NOS-2

nos-2 is a member of the nanos gene family which has been characterized as regulators of germ cell development. *nos-2* mRNA is localized to the P-granules during oogenesis and early embryogenesis, and in somatic blastomeres *nos-2* mRNA is degraded. NOS-2 protein is not expressed until P4 which is a precursor to primordial germ cells. D'Agostino et al (2006) provided evidence that the restriction of NOS-2 protein to the primordial germ cells during early embryogenesis is attributed to the 3' untranslated region. Interestingly, evidence also shows that different conserved fragments of the 3'-UTR are required for different aspects of *nos-2* mRNA regulation. While some fragments needed for *nos-2* mRNA translational repression occur during oogenesis, other fragments needed for translational repression occur during early embryogenesis. More specifically, experimental evidence shows that subA is required for the repression of NOS-2 protein expression in oocytes, while subB and subC are required for repression of NOS-2 protein in the early embryo (Fig. 4).

Experimental evidence indicates that POS-1, an RNA binding protein, is required for the derepression of NOS-2 protein expression in P4, while MEX-5 and MEX-6 are required for nos-

2 mRNA degradation in the somatic blastomeres. Furthermore, POS-1 is not required for NOS-2 expression in P4 when translational repression is absent, which suggests that POS-1 acts as an antagonist to the translation repression. Since POS-1 is expressed in the posterior blastomeres during early embryogenesis clarification is needed on how POS-1 antagonizes translational repression in P4 and not in the precursor cells. D'Agostino et al (2006) provide two speculative mechanisms: the repression of nos-2 translation is weakened after each cell division so that in P4, POS-1 is able to derepress nos-2, or there is an unidentified protein first expressed in P4 that is also required for derepression of nos-2 translation.

5'UAGAAGAUCCAAUUUCUCAAUACUUUUUUAUAUCGGGUCCAAC
CGUUUAUUUUCUACAAGCUUUCACAAACAGATAGUUUAUUGAGU
UACCCGUUCAUAGCCUUUAUUGAUUCCAAAUUUCCCAUCUCACA
CUUUUCUACGGUAUACCAUUUACUUUUUCUGCUAAUAAUCAAUU
AUUAAUACCGUAUAAUGGUCCUCUAUAUUGUCCACGTAACAACUU
GTGCUUUUUCGUCGAAUUUUCAUCAGUUUGUGGAAGAAAGUGAUA
ACUGAAAGAAAGAAGUUU3'

Figure 4: The nos-2 mRNA 3'untranslated region with the following fragments with respect to color subA, subB, subC, subD, subE.

Dr. Sean Ryder's laboratory at UMass Medical School is primarily focused on RNA binding proteins important during early embryogenesis in *C. elegans*. The most recent paper published in the lab focused on the binding specificity of MEX-5. MEX-5 is an RNA-binding protein containing a tandem CCCH Zinc finger domain. Pagano et al (2007), demonstrated that MEX-5 binds to any uridine rich sequence greater than 9 nucleotides. Many mRNA transcripts in *C. elegans* contain 3'-UTR uridine rich sequences, which demonstrates that MEX-5 cannot confer target selection of mRNA. It was also demonstrated that MEX-5 binds to conserved fragments in the *nos-2* and *glp-1* 3'-UTR. More specifically, MEX-5 binds to four fragments of

the temporal control region of the *glp-1* 3'-UTR, and subA, subC, and subE of the *nos-2* 3'-UTR ($K_{d, app}$ ~20-100 nM).

PROJECT OBJECTIVE

Preliminary binding experiments conducted in Dr. Sean Ryder's laboratory before the commencement of my research indicated that *in vitro* the *nos-2* 3' untranslated region is a target of MEX-3 binding. As mentioned above, MEX-3 is localized to P-granules during early embryogenesis, and *nos-2* is translationally repressed via its 3'-UTR and is first derepressed in P4. In MEX-3 mutants, P3 produces daughters that both resemble P4, thus D adopts a P4 like fate (Draper et al., 1996). This suggests that MEX-3 is responsible for segregating and repressing a cell fate determinant in P3 that is important for specifying the P4 fate. It is possible that the cell fate determinant that MEX-3 segregates to P4 is nos-2 and thus the mex-3 mutant phenotype of P3 is attributed to the inability of segregating NOS-2 to P4 exclusively. Due to the aforementioned mex-3 mutant phenotypes and preliminary binding experiments, my research focused on determining MEX-3's binding specificity to the 3'untranslated region of *nos-2* mRNA.

METHODOLOGY

MEX-3 Protein Growth and Purification

pMAL-ac vector containing MEX-3 amino acids 45-205 fused to maltose binding protein was transformed into *Escherichia coli* cells (note: vector also contains ampicillin resistance gene). The *E. col*i were then streaked on an agar plate containing ampicillin to select for positive *E. coli*. The agar plate was incubated overnight at 37°C. One colony was selected from the plate added to 50 mL of LB-Amp, and was incubated at 37°C overnight on the shaker. 5 mL of the starter culture was added to 2X 1 Liter LB-Amp then incubated at 37°C for ~3 hours in a shaker. OD_{600} readings were taken using a spectrophotometer, and induction of protein expression was commenced at 0.6 OD with the addition of 1 mL of 1M IPTG. Incubation and shaking was continued for four hours, then the cells were harvested via centrifugation and the cell pellet was stored at -80°C.

Each cell pellet was resuspended in 50 mL of lysis buffer (50 mM Tris pH 8.0, 200 mM NaCl, 2 mM DTT, 1 EDTA-free protease inhibitor tablet per 50 mL). The pellet was homogenized via repetitive pipetting and then sonicated. The lysate was centrifuged at 8000xg for 20 minutes yielding the clarified lysate. An amylose column was equilibrated with lysis buffer and the clarified lysate was run through it. The protein was eluted using lysis buffer supplemented with maltose (250 mL lysis buffer and 900 mg maltose powder). Fractions were collected, and an SDS-PAGE was run using aliquots of each fraction. Fractions containing MEX-3-MBP fusion protein were pooled and dialyzed overnight in low salt Q-column buffer (50 mM Tris pH 8.8, 20 mM NaCl, 2mM DTT).

An ion exchange Q-column was equilibrated using a low salt Q-column buffer. The amylose elution in low salt Q-column buffer was run through the Q-column. The protein was

eluted using a NaCl gradient starting with 20 mM NaCl to 1M NaCl. The gradient was formed using low salt Q-column buffer (50 mM Tris pH 8.8, 20 mM NaCl, 2 mM DTT) and high salt Q-column buffer (50 mM Tris pH 8.8, 1M NaCl, 2 mM DTT). The protein containing fractions were pooled and dialyzed overnight in low salt S-column buffer (50 mM MOPS pH 6.0, 20 mM NaCl, 2 mM DTT). The Q-column pooled protein fractions in low salt S-column buffer was run through an ion exchange S-column. The S-column was first equilibrated with low salt S-column buffer and the protein was run through the column. The MEX-3 protein was eluted from the column using a NaCl gradient of 20 mM-1M. Low salt S-column buffer (50 mM MOPS pH 6.0, 20 mM NaCl, 2 mM DTT) and high salt S-column buffer (50 mM MOPS pH 6.0, 1M NaCl, 2 mM DTT) were used to establish the salt gradient. The fractions were collected and protein containing fractions were pooled (determined via SDS-PAGE). The pooled protein containing fractions were dialyzed overnight in Eluent A (50 mM Tris pH 8.8, 20 mM NaCl, 2 mM DTT). The pooled protein fractions from the S-column in Eluent A was run through an ion exchange source Q-column. The elution salt gradient was established using Eluent A (50 mM Tris pH 8.8, 20 mM NaCl, 2 mM DTT) and Eluent B (50 mM Tris pH 8.8, 2M NaCl, 2 mM DTT).

After the protein containing fractions were determined via SDS-PAGE, the fractions were pooled and dialyzed overnight in storage buffer. The protein concentration was measured with a spectrophotometer at 280nm and subsequently calculated using the extinction coefficient 70820. The protein was concentrated to 55 μM with a total volume of 4 mL.

RNA Oligo labeling

RNA oligo's of *nos-2* 3'-UTR mRNA were 3'-labeled via fluorescein 5-thiosemicarbazide (Table1). On a fundamental level the reaction occurs by first exposing the

RNA oligo to $NaIO_4$ which results in the oxidation of both the terminal 3'OH and 2'OH to aldehydes. The RNA oligo is then exposed to Fluorescein-5-thiosemicarbazide which contains an amine group that nucleophilically attacks one of the terminal aldehydes on the 3' end of the oligo and forms an imine bond.

Table 1: Series of RNA Oligos 3'fluorescein Labeled Used in Binding Experiments. The underlined and bold portions denote the octomer repeat

First set of RNA oligos	Sequences
nos-2 subA	CAAUACUUUUUUAUAUCGGGUCCAACCGUUUA
nos-2 subB	UACAAGCUUUCACAAACAGATAGUUUAU
nos-2 subC	CCCGUUCAUAGCC**UUUAUUGA**UUCCAAAUUU
nos-2 subD	CCCAUCUCACACUUUUCUACGGUAU
nos-2 subE	ACCAUUUACUUUUUCUGCUAAUAAUCAAUUAUUAAUA
Second set of RNA oligos	
subB/C(C. elegans)	GAUAG**UUUAUUGA**GUUACCCGUUCAUAGCC**UUUAUUGA**UUCCAA
subB/C(C. Briggsae)	CACAU**UUUAUUGA**ACUACAGAAUU**UUUAUUGA**CUGCACCA
subB/C(C. remaniae)	AGAUC**UUUAUUGA**AUCGCUCGCUCAUAGACA**U**C**UAUUGA**UUCCA
Third set of RNA oligos	
subC (mutant 1)	CCCGAAAAUAGCCUUUAUUGAUUCCAAAUUU
subC (mutant 2)	CCCGUUCAUAGCCAAAAUUGAUUCCAAAUUU
subC (mutant 3)	CCCGUUCATAGCCUUUAUUGAAAACAAAUUU
Fourth set of RNA oligos	
nos-2 subC1	CCCGUUCAUAGC
nos-2 subC2	UAGCCUUUAUUG
nos-2 subC3	C**UUUAUUGA**UUC
nos-2 subC4	GAUUCCAAAUUU
nos-2 subC5	CC**UUUAUUGA**UU
nos-2 subC6	CCCGUUCAUAGCCUUU
nos-2 subC7	AUUGAUUCCAAAUUU
nos-2 subC8	GCC**UUUAUUGA**UUCC

Titration Fluorescence Polarization Assay

Titration fluorescence polarization assays (tFP) were conducted using the MEX-3 MBP fusion protein and 3'fluorescein labeled RNA oligos. These assays were conducted in addition

to EMSAs because unlike EMSAs the analysis does not interfere with the equilibrium of the binding reactions since they are measured in solution (Lundblad et al., 1996). To begin these experiments, a master mix was prepared which contained 10X buffer, IGEPAL, tRNA, and 3' fluorescein labeled RNA oligo. The master mix was placed in 60°C water bath for 2 minutes. Three master titrants were then made by diluting MEX-3 to 2 μM. Three separate 2/3 serial dilutions of the master titrants were prepared in a 96 well round bottom plate starting with 2 μM and continuing each dilution series to 23 wells and leaving the 24th well without protein. Master mix was pipetted into 72 wells of a 96 well flat bottom plate. The protein dilution series was pipetted into the 96 well flat bottom plate containing the master mix. The binding reaction was incubated at room temperature (in the dark) for 3 hours to allow equilibration. The fluorescence polarization measurements were made using a Perkin Elmer Multilabel counter. A macro in IGOR was designed to fit the measurements (mP) to the following Hill equation:

$$f = b + \left[\frac{m - b}{1 + 10^{n(\log K_d - \log[P])}} \right]$$

In this equation, m denotes maximum signal, b denotes the base signal, n is the Hill coefficient, K_d is the equilibrium dissociation constant, P is the protein concentration, and f is the fraction bound (Hill, 1910). A graph of the polarization data (mP) verses the protein concentration (logarithmic scale) was made and the Hill equation was fit to the data. From this, the equilibrium dissociation constant of MEX-3-MBP to various fluorescent RNA oligomers was determined.

Electrophoretic Mobility Shift Assays

Each equilibrated sample from the tFP was further analyzed using EMSAs. EMSAs provide the benefit of being able to see the binding, so quantified dissociation constants could be compared to the approximate dissociation constant provided by the gel shift. 1% agarose gels (made with 1X TAE) were used for the shorter RNA oligo's while 5% horizontal polyacrylamide gels (made with 0.5X TBE) were used for the longer RNA oligos (~30 nucleotides). The use of the 5% polyacrylamide for longer RNA oligos alleviated well-shift and resolution problems associated with the agarose gels. Both the agarose gels and polyacrylamide gels were made with three rows of 20 wells, with the last well used for the no protein sample. The agarose gels were run with 1X TAE buffer and the polyacrylamide gels were run with 0.5X TBE buffer for 40 minutes and one hour respectively (120 V). 10 μL of loading dye (bromocresol green) was added to each well containing the equilibrated samples before being loaded into the gel. Each gel was read in a FUJI FLA-500 imager. The dissociation constant was quantified by plotting the fraction bound versus the protein concentration (logarithmic scale) and fitting it to the Hill equation. The fraction bound for each lane was determined by dividing the protein bound RNA signal over the total signal for the lane.

NaCl Dependence of MEX-3 Binding to nos-2 subC

These experiments were essentially performed the same as the fluorescence polarization and electrophoretic mobility shift assays, but with alterations in the NaCl concentration. The following NaCl concentrations in the 10X master mix were used: 2M, 0.5M, 0.25M, and 0M.

RESULTS

Titration Fluorescence Polarization Assay Results

The titration fluorescence polarization assays demonstrated that MEX-3 binds with high affinity to nos-2 subC (Fig. 5), low affinity to subB, and does not bind subA, subD, and subE. The average dissociation constant (three separate measurements) calculated by fitting the data obtained from the fluorescence polarization assay to the Hill equation was ~15 nM for subC, and ~181 nM for subB. The average standard deviation was +/- 0.2 nM and +/- 16 nM respectively. In cases of bimolecular interaction between RNA and protein, the Hill coefficient should be equal to one. Large deviations from one may indicate that the equilibrium was not reached, or there was cooperative binding between multiple proteins. However, small deviations may be attributed to the protein or RNA sticking to the tube in which the binding reaction was contained. The tFP for subC yielded an average Hill coefficient of 1.2 (Table 2).

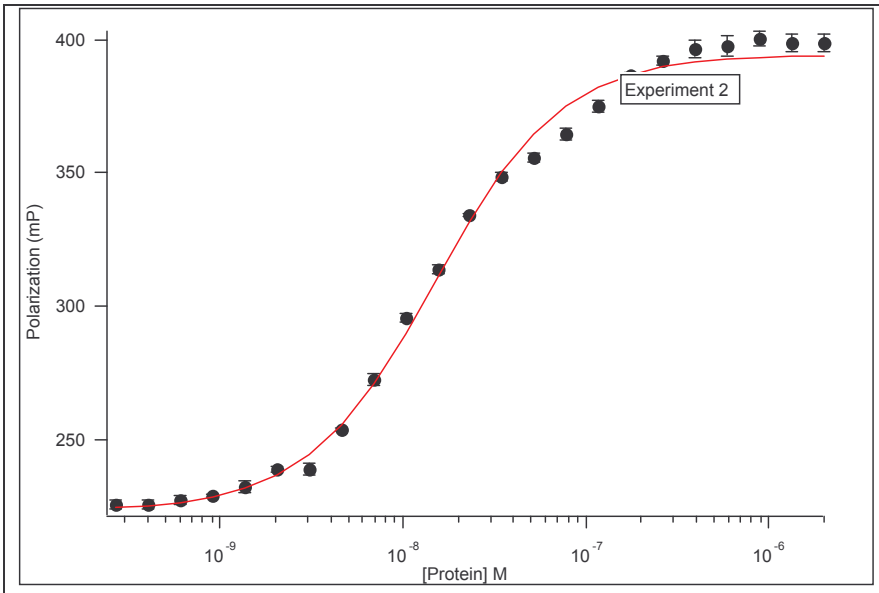

Fig 5: MEX-3 titration into 3'fluorescein labeled nos-2 subC. X-axis indicates MEX-3 concentration, Y-axis indicates polarization, and red line indicates the data points fit to the Hill equation. The error bars show the standard deviations between the five reads taken.

Table 2: Quantification of Dissociation Constant Based on Fitting to Hill Equation.

MEX-3 Titration	Kd	Hill Coefficient
Experiment 1	14.5E-09	1.2
Experiment 2	14.8E-09	1.2
Experiment 3	14.7E-09	1.2
Average	14.7E-09	1.2
St. Dev.	1.5E-10	0

Since MEX-3 bound to *nos-2* subC with the highest affinity, and only weakly to the other conserved fragments, the next step was to further specify the MEX-3 binding site. Sequences that are conserved between species can offer a starting point for finding potential binding sites. Three *nos-2* subB/C oligos from different species (*C. elegans*, *C. briggsae*, *C. remaniae*) were used in the following set of binding experiments. *nos-2* subB/C was used as opposed to subC because it contains an octomer repeat where one of the repeats is located between subB and subC and the other is located within subC. *nos-2* subB/C *C. elegans* and *C. briggsae* both contain two

complete octomer repeats; however, subB/C *C. remaniae* contains one full octomer repeat and one partial octomer repeat (single nucleotide difference). The titration fluorescence polarization assays using the three *nos-2* subB/C RNA oligos demonstrated that MEX-3 binds with negligible change in affinity to *nos-2* subB/C *C. elegans* and *C. briggsae* but reduced affinity to *nos-2* subB/C *C. remaniae* (Fig. 6). The average dissociation constant (three separate measurements) calculated by fitting the data obtained from the tFP to the Hill equation was ~41.8 nM for subB/C *C. remaniae*. The average standard deviation was +/- 1.5 nM. The increase in the dissociation constant represents a ~3-fold decrease in binding when compared to *nos-2* subB/C from the other species. The average Hill coefficient was 1.2 (Table 3).

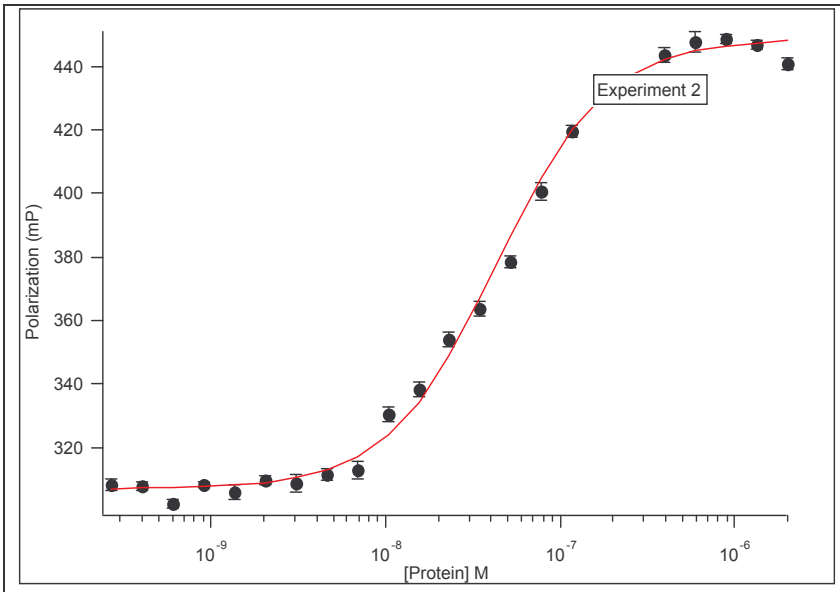

Figure 6: MEX-3 titration into 3'fluorescein labeled nos-2 subB/C *C. remaniae*. X-axis indicates MEX-3 concentration, Y-axis indicates polarization, and red line indicates the data points fit to the Hill equation. The error bars show the standard deviations between the five reads taken.

Table 3: Quantification of Fluorescence Polarization by Fitting to Hill Equation.

MEX-3 Titration	Kd	Hill Coefficient
Experiment 1	41.3E-09	1.2
Experiment 2	43.5E-09	1.4
Experiment 3	40.6E-09	1.0
Average	41.8E-09	1.2
St. Dev.	1.5E-09	.2

Since there was no significant difference in the binding affinity of MEX-3 to subC when compared to the subB/C of *C. elegans,* the minimal binding site was narrowed down to subC. The purpose of the next set of binding experiments was to further specify the MEX-3 binding site by creating mutant *nos-2* subC oligos. Three mutant subC oligos were formed by introducing three nucleotide mutations in separate locations within subC (near the 5' end of oligo, center of oligo, near the 3' end of oligo). A mutant that showed a decrease in MEX-3 binding affinity when compared to wild type subC would indicate a site important for MEX-3 binding. From the previous set of binding experiments it was expected that mutant 2 would show a decrease in MEX-3 binding affinity because the mutation is located within the octomer repeat. A decrease in MEX-3 binding affinity to mutant 2 would also validate that the decrease in binding affinity observed for the subB/C of *C. remaniae* was indeed due to the partial octomer repeat and not other sequence variances between the species. The titration fluorescence polarization assays using the three mutated *nos-2* subC RNA oligos demonstrated that MEX-3 binds with negligible change in affinity to *nos-2* subC mutant 1 and mutant 3, but reduced affinity to mutant 2 (Fig. 7). The average dissociation constant (three separate measurements) calculated by fitting the data obtained from the tFP to the Hill equation was ~58.5nM for subC mutant 2. The average standard deviation was +/- 1.2 nM. The increase in the dissociation constant represents a 4-fold decrease in binding. The average Hill coefficient was 1.2 (Table 4).

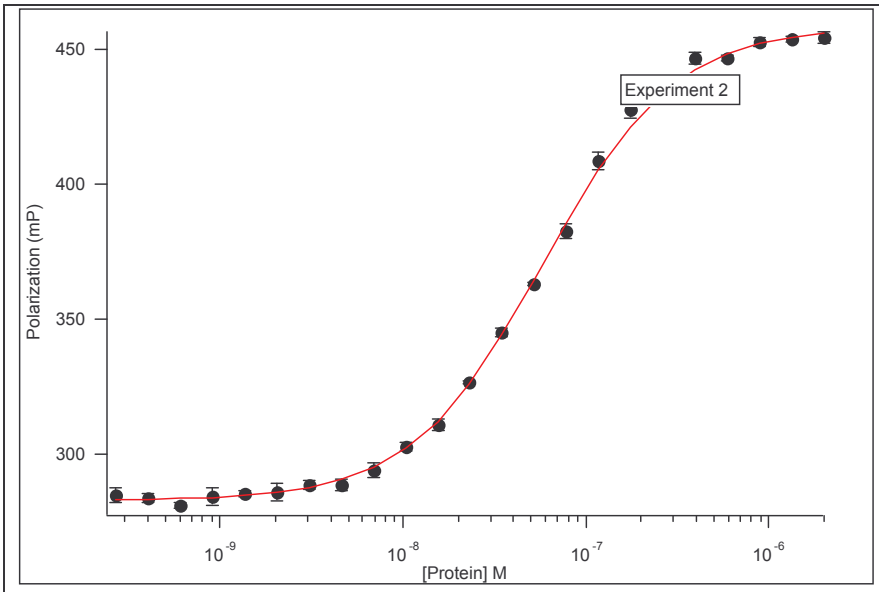

Figure 7: MEX-3 titration into 3'fluorescein labeled nos-2 subC mutant 2. X-axis indicates MEX-3 concentration, Y-axis indicates polarization, and red line indicates the data points fit to the Hill equation. The error bars show the standard deviations between the five reads taken.

Table 4: Quantification of Dissociation Constant Based on Fitting to Hill Equation.

MEX-3 Titration	Kd	Hill Coefficient
Experiment 1	60.2E-09	1.3
Experiment 2	58.7E-09	1.2
Experiment 3	56.5E-09	1.1
Average	58.5E-09	1.2
St. Dev.	1.9E-09	.1

The preceding binding experiments indicated that MEX-3 binds to *nos-2* subC, and that the octomer repeat is of importance for this binding. To further specify the MEX-3 binding site to *nos-2,* subC titration fluorescence polarization experiments were conducted using shortened fragments of *nos-2* subC. The hypothesis was that MEX-3 would bind to the shortened subC

fragment that contains the octomer repeat; however, these experiments (data not shown) indicated that MEX-3 does not bind to any of the shortened subC fragments (>1000 nM Kd).

Electrophoretic Mobility Shift Assay Results

After each titration fluorescence polarization assay (tFP) was conducted, the equilibrated samples were used in electrophoretic mobility shift assays (EMSA). EMSAs provide the experimenter with a visualization of the binding and an approximate dissociation constant. The approximate dissociation constant is the protein concentration where half of the signal (3' labeled RNA olgio) is bound and half is free. EMSAs also allow one to see if there are other shifted species within the equilibrated samples and dissociation of bound protein from RNA. The dissociation constant for MEX-3 binding to *nos-2* subC was determined by plotting the fraction of bound RNA versus the protein concentration and fitting the data to the Hill equation (Fig. 8). The dissociation constant, determined from the average of three experiments, was 18.1E-09 nM +/- .6E-09 nM (Table 5). This value is close to the value obtained from tFP which was 14.7E-09 nM +/- .15E-09 nM. The average Hill coefficient is 1.3.

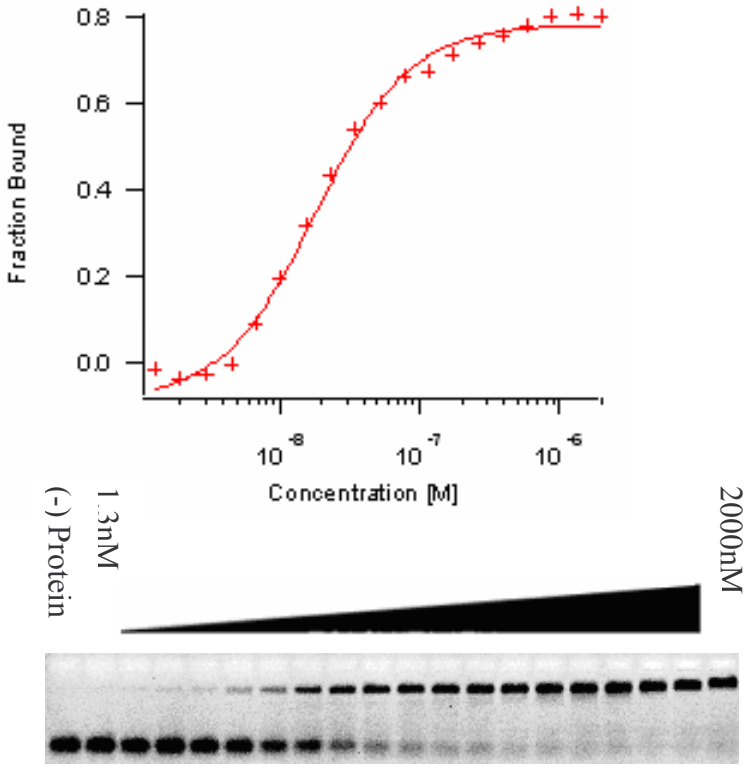

Figure 8: Electrophoretic mobility shift assay of MEX-3 in 3'fluorescein labeled *nos-2* subC. The graph is fraction of bound RNA versus protein concentration. The fraction of bound RNA was determined by dividing the fraction of bound RNA signal by the total signal in the lane. The X-axis indicates the protein concentration, the Y-axis indicates the fraction of bound RNA, and the red line is the data fit to the Hill equation.

Table 5: Quantification of EMSA Data by Fitting to Hill Equation.

MEX-3 Titration	Kd	Hill Coefficient
Experiment 1	18.6E-09	1.3
Experiment 2	17.4E-09	1.2
Experiment 3	18.2E-09	1.3
Average	18.1E-09	1.3
St. Dev.	6.0E-10	.1

EMSAs were also conducted for the nos-2 subB/C oligos for each species. The respective dissociation constants for MEX-3 binding to nos-2 subB/C were determined in the aforementioned manner. The EMSAs indicated that MEX-3 binding affinity was only significantly weakened by the nos-2 subB/C of *C. remaniae* (Fig. 9). The dissociation constant, determined from the average of three experiments, was 60.2-09 nM +/- 17.4E-09 nM (Table 6). This value deviates significantly from the value obtained from tFP which was 41.8E-09 +/- 1.5E-

09. As a result, the change in binding affinity between the subB/C of *C. elegans* and the subB/C of *C. remaniae*, as determined via EMSA, is approximately a 4-fold decrease, and only ~2-fold decrease as determined by tFP. This deviation may be attributed to the disruption of the equilibrium upon loading the EMSA. The average Hill coefficient is 1.4.

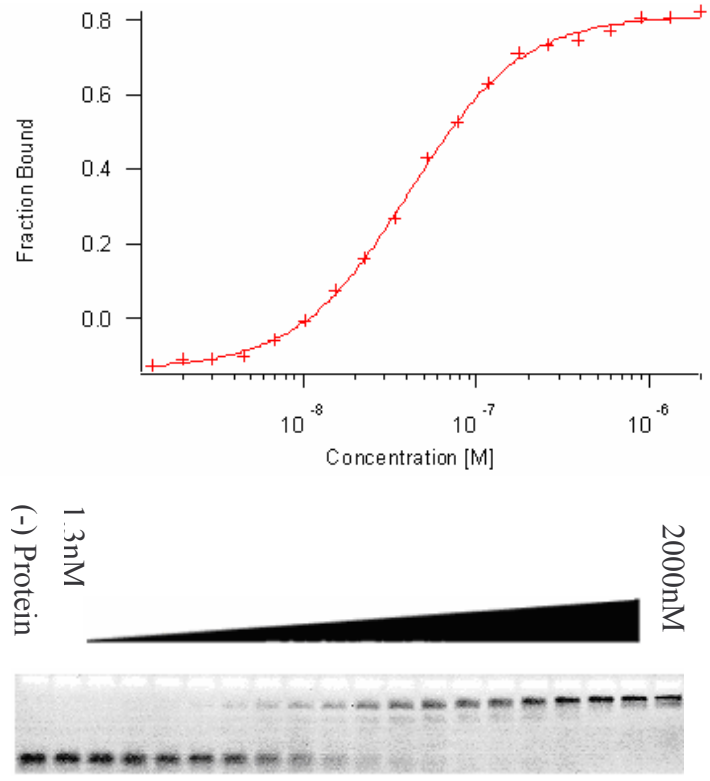

Figure 9: Electrophoretic mobility shift assay of MEX-3 in 3'fluorescein labeled *nos-2* subB/C *C. remaniae*. The graph is fraction of bound RNA verses protein concentration. The X-axis indicates the protein concentration, the Y-axis indicates the fraction of bound RNA, and the red line is the data fit to the Hill equation.

Table 6: Quantification of EMSA Data by Fitting to Hill Equation.

MEX-3 Titration	Kd	Hill Coefficient
Experiment 1	41.2E-09	1.3
Experiment 2	63.8E-09	1.3
Experiment 3	75.5E-09	1.5
Average	60.2E-09	1.4
St. Dev.	17.4E-09	.1

EMSAs were also conducted for the *nos-2* subC mutants. The respective dissociation constants for MEX-3 binding to *nos-2* subC mutants were determined in the aforementioned manner. The EMSAs indicated that MEX-3 binding affinity was only significantly weakened by the *nos-2* subC mutant 2 (Fig. 10). The dissociation constant, determined from the average of three experiments, was 107E-09 nM +/- 18.9E-09 nM (Table 7). This value significantly deviates from the value obtained from tFP which was 58.5E-09 nM +/- 1.9E-09 nM. As a result, the change in binding affinity between subC and subC mutant 2, as determined via EMSA, is approximately a 6-fold decrease, and only ~4-fold decrease as determined by tFP. This deviation may be attributed to the disruption of the equilibrium upon loading the EMSA. The average Hill coefficient is 1.3.

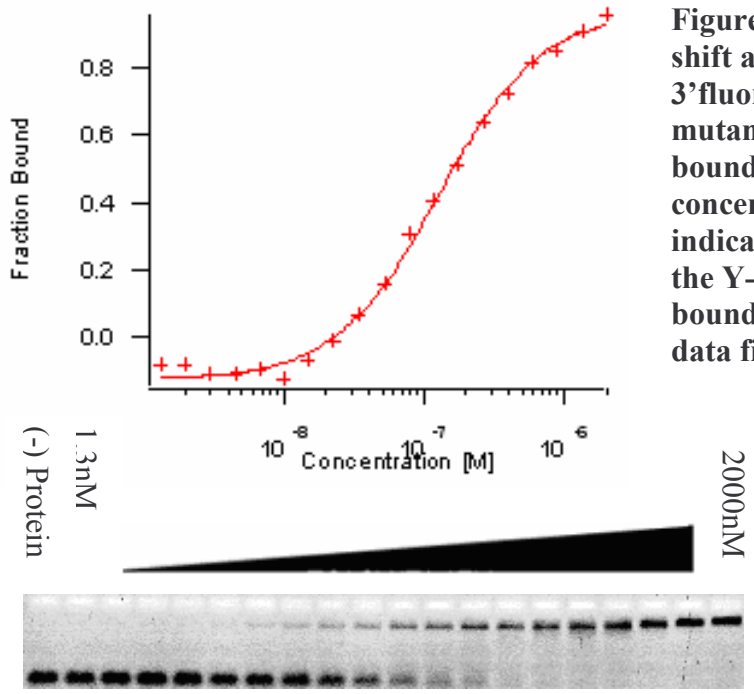

Figure 10: Electrophoretic mobility shift assay of MEX-3 in 3'fluorescein labeled *nos-2* subC mutant 2. The graph is fraction of bound RNA verses protein concentration. The X-axis indicates the protein concentration, the Y-axis indicates the fraction of bound RNA, and the red line is the data fit to the Hill equation.

Table 7: Quantification of EMSA data by fitting to Hill equation

MEX-3 Titration	Kd	Hill Coefficient
Experiment 1	89.4E-09	1.4
Experiment 2	104.6E-09	1.3
Experiment 3	126.9E-09	1.2
Average	107E-09	1.3
St. Dev.	18.9E-09	.1

The EMSA experiments conducted with all shortened fragments of *nos-2* subC (data not shown) indicated that MEX-3 does not bind to any of them which agrees with the titration fluorescence polarization assays (>1000 nM Kd).

NaCl Dependence of MEX-3 Binding to nos-2 subC Results

Titration fluorescence polarization experiments were conducted to test MEX-3's affinity to *nos-2* subC under various NaCl concentrations. The results indicated that NaCl concentrations lower than 50 mM result in significant decreases in MEX-3 affinity to *nos-2* subC (Fig. 11). This is surprising because MEX-3 binds RNA via two KH-domains which have been demonstrated to interact with RNA via hydrophobic amino acid residues, meaning that a change in salt concentration should not alter the protein's binding affinity to RNA (Grishin, 2001). The higher salt concentrations may stabilize RNA secondary structure that is favorable for MEX-3 binding due to bringing two binding domains in proximity optimal for MEX-3 binding. EMSA experiments were also conducted using the same equilibrated samples. The EMSA experiments with NaCl concentrations below 50 mM were not quantifiable because they showed two distinct bound species (Fig. 12).

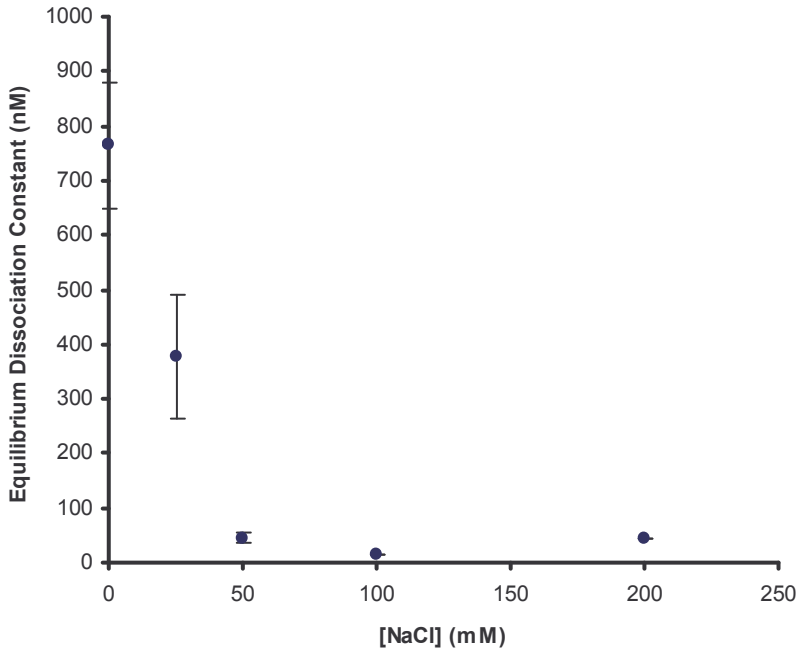

Figure 11: [NaCl] dependence of MEX-3 affinity to *nos-2* subC was determined through titration fluorescence polarization. From 200 mM NaCl to 50 mM NaCl deviations in NaCl do not result in deviations in affinity; however, from 50 mM to 0 mM there is a large decrease in affinity of MEX-3 for subC.

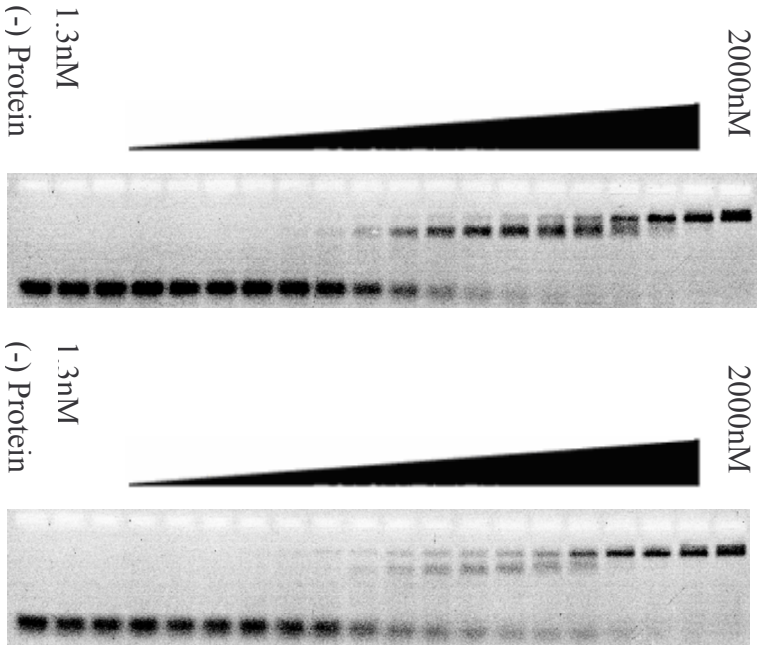

Figure 12: Electrophoretic mobility shift assay of MEX-3 in 3'fluorescein labeled *nos-2* subC. Top gel 0 mM NaCl and bottom gel 25 mM NaCl. The gels were not quantifiable due to the formation of two distinct bound species.

DISCUSSION

The results obtained from the titration fluorescence polarization assays and electrophoretic mobility shift assays for each conserved fragment of the *nos-2* 3'UTR characterized in the literature (subA through subE) indicates that MEX-3 only binds to *nos-2* subC with high affinity. There is only a marginal difference in the dissociation constant obtained from both assays. The results obtained from the *nos-2* subB/C oligos from different species provided evidence that the octomer repeat was part of the MEX-3 binding site since the *C. remaniae* fragment contained both a full octomer repeat and a partial octomer repeat and there was a decrease in MEX-3 binding affinity. It could not be concluded at that time whether it was the partial octomer repeat that caused the decrease in MEX-3 binding affinity because there were other sequence variances between the different species. There is only a marginal difference between MEX-3 binding affinity to the nos-2 subB/C of *C. elegans* and the *nos-2* subC of *C. elegans* which indicated that the subC fragment was the minimal binding fragment elucidated at that point in progress. The discrepancy between the binding affinities obtained from EMSAs (4-fold decrease in binding) and tFPs (2-fold decrease in binding) may be attributed to a perturbation of the equilibrium during EMSA loading.

The experiments conducted using the mutated *nos-2* subC fragments validated that the octomer repeat is part of the MEX-3 binding site since only the mutant with a mutation in the octomer repeat showed a decrease in MEX-3 binding affinity. As with the preceding experiment, the discrepancy between the binding affinity determined by EMSA (6-fold decrease in binding) and tFP (4-fold decrease in binding) could have been caused by a perturbation of the equilibrium during EMSA loading. The complete lose of MEX-3 binding to *nos-2* subC upon shortening the

RNA to smaller fragments was demonstrated by both the EMSAs and tFPs. These results indicate that the entire *nos-2* subC is required for MEX-3 binding.

The binding experiments testing for MEX-3 binding dependence on NaCl indicates that MEX-3 binding affinity to *nos-2* subC is significantly decreased in conditions where NaCl concentrations are below 50 mM. This was unexpected due to the fact that MEX-3 binds to RNA via hydrophobic interactions (Grishin, 2001). The data obtained from the EMSAs was not quantifiable due to the formation of two distinct bound fractions in the lower salt concentrations. The secondary structure of *nos-2* subC may be stabilized under higher salt concentrations and thus the secondary structure is unstable under the lower salt concentrations. This indicates the possibility that MEX-3 binding to *nos-2* subC is contingent upon a stabilized secondary structure. The two distinct bound fractions shown by the EMSAs may be attributed to an equilibrium between *nos-2* subC without secondary structure, and *nos-2* subC with secondary structure. This would mean that the lower bound fraction would be MEX-3 binding to subC without secondary structure and the higher bound fraction would be MEX-3 binding to subC with secondary structure since secondary structure would impede movement through the gel. The gels provide some support for this idea because under 0 mM salt concentration there is a significantly larger signal for the lower bound fraction and a significantly lower signal for the higher bound fraction which coincides with a greater amount of *nos-2* subC without secondary structure. Conversely, under 25 mM salt concentration there is a much weaker lower signal for the lower bound fraction than the higher bound fraction which coincides with a greater amount of *nos-2* subC with secondary structure. Furthermore, under 100 mM salt (concentration used for other experiments) the lower bound fraction is completely lost which coincides with all of the *nos-2* subC containing a stabilized secondary structure.

Although, the results indicate that MEX-3 binds to *nos-2* subC, this does not provide evidence that MEX-3 behaves the same way *in vivo* and acts as regulator of *nos-2* expression during early embryogenesis in *C. elegans*. Subsequent experiments should be first oriented towards further specifying MEX-3's binding specificity to *nos-2* subC. For example, an RNA footprinting experiment for MEX-3 binding to *nos-2* subC would show the location of MEX-3 binding to *nos-2* subC, thus narrowing down the site of binding. Following RNA footprinting, experiments testing change in binding affinity by creating mutant *nos-2* subC's with mutations located in the center of the oligo moving outward would possibly reveal the location of binding sites for each KH domains.

After determining MEX-3's binding specificity to *nos-2* subC *in vitro*, *in vivo* experiments oriented towards testing MEX-3's role as a post-transcriptional regulator of *nos-2* should be conducted. For example, wild type expression of NOS-2 protein could be compared to *C. elegans* with mutations specific for the MEX-3 binding site that was determined through the *in vitro* experiments. The resulting NOS-2 protein expression could be compared to NOS-2 protein expression in MEX-3 knockdowns.

BIBLIOGRAPHY

Bowerman, B. (1998). Maternal control of pattern formation in early *Caenorhabditis elegans* embryos. *Curr. Top. Dev. Biol*. 39, 73-117.

D'Agostino, I., Merritt, C., Chen, P. L., Seydoux, G., Subramaniam, K. (2006). Translational repression restricts expression of the *C. elegans* Nanos homolog NOS-2 to the embryonic germline. *Developmental Biology* 292, 244-252.

Draper, B. W., Mello, C. C., Bowerman, B., Hardin, J., and Priess, J. R. (1996). MEX-3 Is a KH Domain Protein That Regulates Blastomere Identity in Early *C. elegans* Embryos. *Cell* 87, 205-217.

Grishin, N. V. (2001). KH domain: one motif, two folds. *Nucleic Acids Research* 29, 638-643.

Hill, A. V. (1910). The possible effects of the aggregation of the molecules of hemoglobin on its oxygen dissociation curve. *J Physiol*. (London) 40, 4-7.

Huang, N. N., Mootz, D. E., Walhout, A. J. M., Vidal, M., Hunter, C. P. (2002). MEX-3 interacting proteins link cell polarity to asymmetric gene expression in Caenorhabditis elegans. *Development* 129, 747-759.

Hunter, C.P., and Kenyon, C (1996). Spatial and temporal controls target pal-1 blastomere-specification activity to a single blastomere lineage in *C. elegans* embryos. *Cell* 87, 217-226.

Kuersten, S., and Goodwin, E. B. (2003). The Power of the 3'UTR: Translational Control and Development. *Nature Review Genetics* 4, 626-637.

Lundblad, J. R., Laurance, M., and Goodman, R. H. (1996). Fluorescence Polarization Analysis of Protein-DNA and Protein-Protein Interactions. *Molecular Endocrinology* 10, 607-612.

Mootz, D., Ho, D. M., Hunter, C. P. (2004). The STAR/Maxi-KH domain protein GLD-1 mediates a developmental switch in the translational control of *C. elegans* PAL-1. *Development* 131, 3263-3272.

Pagano, J. M., Farley, B. M., McCoig, L. M., Ryder, S. P. (2007). Molecular Basis of RNA Recognition by the Embryonic Polarity Determinant MEX-5. *Journal of Biological Chemistry* 282, 8883-8894.

Schubert, C. M., Lin, R., de Vries, C. J., Plasterk, R. H., and Priess, J. R. (2000). MEX-5 and MEX-6 function to establish soma/germline asymmetry in early *C. elegans* embryos. *Mol. Cell* 5, 671-682.

Seydoux, G., and Braun, R. E. (2006). Pathway to Totipotency: Lessons from Germ Cells. *Cell* 127, 891-904.

Waring, D. A. and Kenyon, C. (1990). Selective silencing of cell communication influences anteroposterior pattern formation in C. elegans. *Cell* 60, 123-131.

Wormbook: The Online Review of C. elegans Biology. Pasadena (CA): Wormbook; c2005.